Article ID:1673-2049(2006)02-0009-11

Plastic Analysis of Frames with Tapered Members

W. S. King[1], C. J. Chen[1], L. Duan[2], W. F. Chen[3]

(1. Department of Construction Engineering, Chaoyang University of Technology, Wufeng 00886, Taiwan, China;
2. Department of Traffic Engineering, University of California, Sacramento CA95816, California, USA;
3. School of Engineering, University of Hawaii, Honolulu HI96822, Hawaii, USA)

Abstract: Several in-plane tapered members were analyzed by the simple plastic hinge method. The stiffness matrix of an I-section tapered element was derived by the finite element method with the use of superposition principle. In order to predict the locations of plastic hinges formation in members, an element subjected to bending moments and an axial load was modeled to simulate these tapered members with different boundary conditions. An additional nodal point was set after the formation of a plastic hinge was detected within the element. The most reasonable load and deflection curve could be obtained by using the two elements for each member. One should pay attention to the problem of direction in the stiffness matrix of a tapered element. The actual limit load of a beam-column could not be predicted correctly if the possible formation of a plastic hinge in a member was not considered. The limit load would be overestimated if only one element was used for a tapered member. The results show that the proposed method can be reasonably applied to the plastic analysis of frames with tapered members.

Key words: tapered member; beam-column element; plastic hinge; structural engineering; steel
CLC number: TU313.2 **Document code**: A

采用楔形构件框架的塑性分析

W. S. King[1], C. J. Chen[1], L. Duan[2], W. F. Chen[3]

(1. 朝阳科技大学 结构工程系,中国台湾 雾峰 00886; 2. 加利福尼亚大学 交通工程系,加利福尼亚 萨克拉曼多 CA95816; 3. 夏威夷大学 工程学院,夏威夷 火奴鲁鲁 HI96822)

摘要: 对一些平面内楔形截面构件进行二阶简单塑性铰法分析,并利用有限元法及重叠原理推导I形钢楔形截面构件的刚度矩阵。为预测构件内部可能形成塑性铰的位置,以一个同时受弯矩及轴力作用的梁柱单元,仿真各种不同边界条件的楔形截面构件。若预测构件内会形成塑性铰的位置则要增设一个节点,将一个构件分割为两个单元,以获得最合理的荷载-挠度曲线。楔形截面构件的刚度矩阵应特别注意方向性的问题。若没有考虑到任一构件中可能形成塑性铰的位置,就不能准确地预测梁柱真实的极限承载能力。若仅用一个单元代表一个楔形截面构件就会高估极限承载能力。该方法可合理地应用于具有楔形截面构件框架的塑性分析。

关键词: 楔形构件;梁柱单元;塑性铰;结构工程;钢结构

Received date: 2006-04-23

Biography: W. S. King(1971-), male, Taiwan, China, professor, PhD, E-mail: wonsunking@yahoo.com.cn.

0 Introduction

Tapered members are used popularly in engineering structures, such as ships, automobiles, airplanes, cranes, bridges, and building frames. Tapered members can save materials, reduce dead weight, and beautify the shape of structures. Researches about plastic analyses of tapered members have been reported in the past[1-3]. However, most of those studies focus on the elastic behavior of tapered members due to difficulties in obtaining limit load of a frame with tapered members.

If we can find the location of a plastic hinge in any member exactly, then, we will precisely know both the collapse mechanism and the limit load of a steel frame with tapered members. The location of a plastic hinge formed in a tapered beam-column is not easy to predict. Although we can always determine locations of plastic hinges in a tapered element by the finite element method through setting many fine meshes, it is too tedious by doing so for a framed structure with many tapered members.

If we know the locations of a plastic hinge previously, we can stiffen or repair the structure easily. If we let plastic hinges occur in minor members on purpose, and prevent main members to form plastic hinges, then, we probably can protect the structure when it is subjected to an extreme loading. Hence, we may call these plastic hinges as "artificial plastic hinges" or "guided plastic hinges" for protecting structures.

A simple method to predict the location of plastic hinge in a linearly tapered I-shaped beam-column is established by the authors in the first part of this paper. The plastic analysis of steel frames with tapered members is then carried out in the later part of this paper.

1 Formulation of Mathematical Model

The stiffness matrix of a tapered beam-column having a rectangular section is developed first. We can get the stiffness matrix of a tapered beam-column that has the I-shape section and the same width by superposing three stiffness matrixes of rectangular sections. In other words, by subtracting two small rectangular sections from the whole rectangular section as shown in Fig. 1, we can get the stiffness matrix for a tapered beam-column of I-shape section.

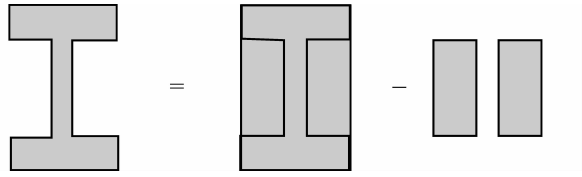

Fig. 1 Stiffness Matrix of I-Shape Cross Section Superposed from That of Three Rectangular Cross Sections

图 1 工形截面刚度矩阵由 3 个矩形截面刚度矩阵叠加合成

The stiffness matrix may degrade when both ends of an element are partially plastic. Based on the method proposed in Reference [4], the stiffness matrix of a beam-column element with a small head and a big tail as shown in Fig. 2 is obtained as Eq. (1).

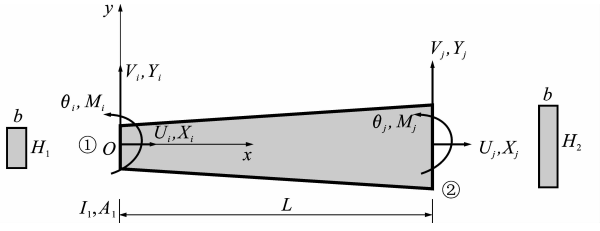

Fig. 2 Six Degree of Freedom in Tapered Element with Small Head and Big End

图 2 楔形单元的六自由度

I_1 is moment of inertia of cross section at the small end; A_1 is area of cross section at the small end.

The stiffness matrix of a beam-column element with a big head and a small tail as shown in Fig. 3 is written in Eq. (2).

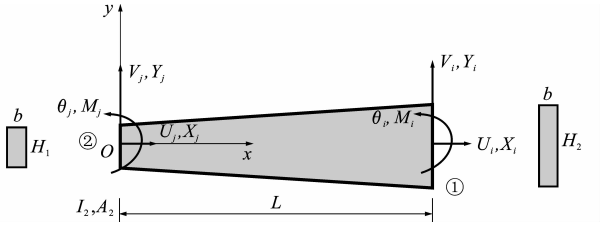

Fig. 3 Six Degree of Freedom in Tapered Element with Big Head and Small End

图 3 倒楔形单元的六自由度

I_2 is moment of inertia of cross section at the big end; A_2 is area of cross section at the big end.

$$\boldsymbol{K}=\begin{bmatrix} \frac{E(A_{H_1}D_1-A_{h_1}D_2)}{L} & & & & & \\ 0 & \frac{S'_{ii}+2S'_{ij}+S'_{jj}}{L^2}+\frac{P}{L} & & \text{sym.} & & \\ 0 & \frac{W'_{ii}+W'_{ij}}{L} & T'_{ii} & & & \\ -\frac{E(A_{H_1}D_1-A_{h_1}D_2)}{L} & 0 & 0 & \frac{E(A_{H_1}D_1-A_{h_1}D_2)}{L} & & \\ 0 & -\frac{S'_{ii}+2S'_{ij}+S'_{jj}}{L^2}-\frac{P}{L} & -\frac{W'_{ii}+W'_{ij}}{L} & 0 & \frac{S'_{ii}+2S'_{ij}+S'_{jj}}{L^2}+\frac{P}{L} & \\ 0 & \frac{Q'_{ij}+Q'_{jj}}{L} & V'_{ij} & 0 & -\frac{Q'_{ij}+Q'_{jj}}{L} & U'_{jj} \end{bmatrix} \tag{1}$$

$$\boldsymbol{K}=\begin{bmatrix} \frac{E(A_{H_1}D_1-A_{h_1}D_2)}{L} & & & & & \\ 0 & \frac{S'_{ii}+2S'_{ij}+S'_{jj}}{L^2}+\frac{P}{L} & & \text{sym.} & & \\ 0 & -\frac{Q'_{ii}+Q'_{ij}}{L} & U'_{ii} & & & \\ -\frac{E(A_{H_1}D_1-A_{h_1}D_2)}{L} & 0 & 0 & \frac{E(A_{H_1}D_1-A_{h_1}D_2)}{L} & & \\ 0 & -\frac{S'_{ii}+2S'_{ij}+S'_{jj}}{L^2}-\frac{P}{L} & \frac{Q'_{ii}+Q'_{ij}}{L} & 0 & \frac{S'_{ii}+2S'_{ij}+S'_{jj}}{L^2}+\frac{P}{L} & \\ 0 & -\frac{W'_{ij}+W'_{jj}}{L} & V'_{ij} & 0 & \frac{W'_{ij}+W'_{jj}}{L} & T'_{jj} \end{bmatrix} \tag{2}$$

All these terms in Eq. (1) and Eq. (2) are explained as follows

$$\left.\begin{aligned} S'_{ii}&=(S'_{33}-S'_{36}\frac{S'_{36}}{S'_{66}}\rho_2)(1-\rho_1)\\ S'_{ij}&=S'_{ji}=S'_{36}(1-\rho_2)(1-\rho_1)\\ S'_{jj}&=(S'_{66}-S'_{63}\frac{S'_{63}}{S'_{33}}\rho_1)(1-\rho_2) \end{aligned}\right\} \tag{3}$$

$$\left.\begin{aligned} S'_{33}&=S'_{66}=\frac{4EI_{H_1}}{L}C_{11}-\frac{4EI_{h_1}}{L}C_{111}+\frac{2PL}{15}+\frac{44P^2L^3}{25\,000EI_1}\\ S'_{36}&=S'_{63}=\frac{2EI_{H_1}}{L}C_{11}-\frac{2EI_{h_1}}{L}C_{111}-\frac{PL}{30}-\frac{26P^2L^3}{25\,000EI_1} \end{aligned}\right\} \tag{4}$$

$$\left.\begin{aligned} T'_{ii}&=(T'_{33}-T'_{36}\frac{T'_{36}}{T'_{66}}\rho_2)(1-\rho_1)\\ T'_{ij}&=T'_{ji}=T'_{36}(1-\rho_2)(1-\rho_1)\\ T'_{jj}&=(T'_{66}-T'_{63}\frac{T'_{63}}{T'_{33}}\rho_1)(1-\rho_2) \end{aligned}\right\} \tag{5}$$

$$\left.\begin{aligned} T'_{33}&=T'_{66}=\frac{4EI_{H_1}}{L}C_{22}-\frac{4EI_{h_1}}{L}C_{221}+\frac{2PL}{15}+\frac{44P^2L^3}{25\,000EI_1}\\ T'_{36}&=T'_{63}=\frac{2EI_{H_1}}{L}C_{22}-\frac{2EI_{h_1}}{L}C_{221}-\frac{PL}{30}-\frac{26P^2L^3}{25\,000EI_1} \end{aligned}\right\} \tag{6}$$

$$\left.\begin{aligned} U'_{ii}&=(U'_{33}-U'_{36}\frac{U'_{36}}{U'_{66}}\rho_2)(1-\rho_1)\\ U'_{ij}&=U'_{ji}=U'_{36}(1-\rho_2)(1-\rho_1)\\ U'_{jj}&=(U'_{66}-U'_{63}\frac{U'_{63}}{U'_{33}}\rho_1)(1-\rho_2) \end{aligned}\right\} \tag{7}$$

$$\left.\begin{aligned} U'_{33}&=U'_{66}=\frac{4EI_{H_1}}{L}C_{44}-\frac{4EI_{h_1}}{L}C_{441}+\frac{2PL}{15}+\frac{44P^2L^3}{25\,000EI_1}\\ U'_{36}&=U'_{63}=\frac{2EI_{H_1}}{L}C_{44}-\frac{2EI_{h_1}}{L}C_{441}-\frac{PL}{30}-\frac{26P^2L^3}{25\,000EI_1} \end{aligned}\right\} \tag{8}$$

$$\left.\begin{aligned} Q'_{ii}&=(Q'_{33}-Q'_{36}\frac{Q'_{36}}{Q'_{66}}\rho_2)(1-\rho_1)\\ Q'_{ij}&=Q'_{ji}=Q'_{36}(1-\rho_2)(1-\rho_1)\\ Q'_{jj}&=(Q'_{66}-Q'_{63}\frac{Q'_{63}}{Q'_{33}}\rho_1)(1-\rho_2) \end{aligned}\right\} \tag{9}$$

$$\left.\begin{aligned} Q'_{33}&=Q'_{66}=\frac{4EI_{H_1}}{L}C_{41}-\frac{4EI_{h_1}}{L}C_{411}+\frac{2PL}{15}+\frac{44P^2L^3}{25\,000EI_1}\\ Q'_{36}&=Q'_{63}=\frac{2EI_{H_1}}{L}C_{41}-\frac{2EI_{h_1}}{L}C_{411}-\frac{PL}{30}-\frac{26P^2L^3}{25\,000EI_1} \end{aligned}\right\} \tag{10}$$

$$\left.\begin{aligned} W'_{ii}&=(W'_{33}-W'_{36}\frac{W'_{36}}{W'_{66}}\rho_2)(1-\rho_1)\\ W'_{ij}&=W'_{ji}=W'_{36}(1-\rho_2)(1-\rho_1)\\ W'_{jj}&=(W'_{66}-W'_{63}\frac{W'_{63}}{W'_{33}}\rho_1)(1-\rho_2) \end{aligned}\right\} \tag{11}$$

$$\left.\begin{aligned} W'_{33}=W'_{66}&=\frac{4EI_{H_1}}{L}C_{21}-\frac{4EI_{h_1}}{L}C_{211}+\frac{2PL}{15}+\frac{44P^2L^3}{25\,000EI_1}\\ W'_{36}=W'_{63}&=\frac{2EI_{H_1}}{L}C_{21}-\frac{2EI_{h_1}}{L}C_{211}-\frac{PL}{30}-\frac{26P^2L^3}{25\,000EI_1}\end{aligned}\right\}\quad(12)$$

$$\left.\begin{aligned} V'_{ii}&=(V'_{33}-V'_{36}\frac{V'_{36}}{V'_{66}}\rho_2)(1-\rho_1)\\ V'_{ij}&=V'_{ji}=V'_{36}(1-\rho_2)(1-\rho_1)\\ V'_{jj}&=(V'_{66}-V'_{63}\frac{V'_{63}}{V'_{33}}\rho_1)(1-\rho_2)\end{aligned}\right\}\quad(13)$$

$$\left.\begin{aligned} V'_{33}=V'_{66}&=\frac{4EI_{H_1}}{L}C_{42}-\frac{4EI_{h_1}}{L}C_{421}+\frac{2PL}{15}+\frac{44P^2L^3}{25\,000EI_1}\\ V'_{36}=V'_{63}&=\frac{2EI_{H_1}}{L}C_{42}-\frac{2EI_{h_1}}{L}C_{421}-\frac{PL}{30}-\frac{26P^2L^3}{25\,000EI_1}\end{aligned}\right\}\quad(14)$$

Where

$$\left.\begin{aligned} r_1&=\frac{H_2}{H_1}-1\\ D_1&=1+r_1(1/2)\\ C_{11}&=1+3r_1(1/2)+3r_1^2(2/5)+r_1^3(7/20)\\ C_{21}&=1+3r_1(1/3)+3r_1^2(7/30)+r_1^3(1/5)\\ C_{22}&=1+3r_1(1/4)+3r_1^2(2/15)+r_1^3(1/10)\\ C_{41}&=1+3r_1(2/3)+3r_1^2(17/30)+r_1^3(1/2)\\ C_{42}&=1+3r_1(1/2)+3r_1^2(13/30)+r_1^3(2/5)\\ C_{44}&=1+3r_1(3/4)+3r_1^2(19/30)+r_1^3(11/20)\end{aligned}\right\}\quad(15)$$

ρ_1, ρ_2 are stiffness decay factors of cross section at an element's ends 1 and 2 respectively.

In the simple plastic hinge method, ρ_1 and ρ_2 jump from zero to one directly. It means that the partially plastic effect in sections is not taken into account in this study.

Some important symbols shown in Fig. 4 are interpreted as follows:

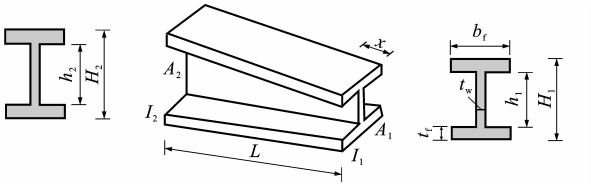

Fig. 4 Linearly Tapered Element of I-Shape Section with Constant Width

图 4 变高度楔形单元

I_1 is moment of inertia of the small end's cross section in a tapered element; I_2 is moment of inertia of the big end's cross section in a tapered element; I_{H_1} is moment of inertia of a whole rectangular cross section at the small end in a tapered element using for superposition; I_{h_1} is moment of inertia of two small rectangular cross sections at the small end in a tapered element using for subtracting superposition; I_{H_2} is moment of inertia of a whole rectangular cross section at the big end in a tapered element using for superposition; I_{h_2} is moment of inertia of two small rectangular cross sections at the big end in a tapered element using for subtracting superposition. x is between 0 and L.

These coefficients C_{111}, C_{211}, C_{221}, C_{411}, C_{421}, C_{441}, and D_2 are the same as those coefficients in Eq. (15) by replacing r_1 with r_2, $r_2=(h_2/h_1)-1$. When $r_1=0$ and $r_2=0$, these stiffness matrixes in Eq. (1) and Eq. (2) become the stiffness matrix of a uniform element. The parameter r_1 in Eq. (15) is equal to r for the solid rectangular section of a tapered element.

2 Limit Surface and Initial Yielding Surface

The limit surface for a wide flange section bent in strong axis is written as[5]

$$(\frac{P}{P_{yx}})^{1.3}+\frac{M_x}{M_{px}}=1\quad(16)$$

The initial yielding surface for a strong axis bending neglecting residual stress is shown in Fig. 5 and is written as[6]

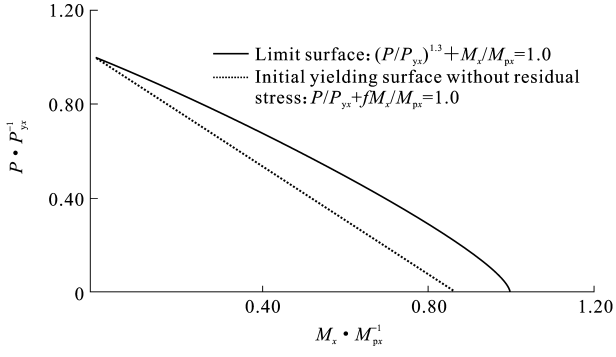

Fig. 5 Initial Yielding Surface and Limit Surface of I-Shape Section

图 5 工形截面初始屈服面和极限屈服面

$$\frac{P}{P_{yx}}+\frac{fM_x}{M_{px}}=1\quad(17)$$

where P is axial load applied in the element; P_{yx} is squash load at a distance of x from the small end; M_x is bending moment at a distance of x from the small end; M_{px} is plastic moment at a distance of x

from the small end; f is shape factor.

These above equations are used for the I-shape section.

3 Coordinate Transformation Matrix and Axial Force

Because a tapered element has a big end and a small end, the stiffness matrix has its own direction. When the local stiffness matrix transfers to the global stiffness matrix, the coordinate transformation matrix has to be dealt with carefully. The angle between the horizontal direction and the inclined direction of a tapered element as shown in Fig. 6 can be measured either at the small end or at the big end. However, the angle is measured at the small end of a tapered element in this paper. When the compressive axial force P is taken from the calculation process in a computer program, it should be careful either in the type of a big-head-small-end element or in the type of a small-head-big-end element. Therefore, the stiffness degradation principle of a cross section at each end of an element can be satisfied[7].

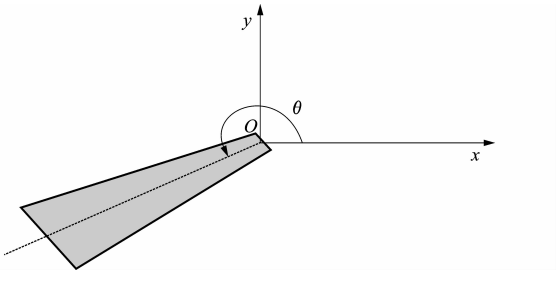

Fig. 6　Angle θ Measured at Small End of Tapered Element in Coordinate Transformation Matrix

图 6　坐标变换矩阵中楔形单元小头端 θ 值

4 Mathematical Model for Predicting the Location of Plastic Hinge

When the most possible location of plastic hinge is predicted, one element of beam-column will be then divided into two elements by adding a new nodal point at this possible location. Hence, we can use the fewer elements to form a reasonable load and deflection curve. The following method is proposed herein to predict the possible location of a plastic hinge in a tapered member.

Two equations defined by Gere[8] are shown below

$$I_x = I_1\left[1+\left(\frac{H_2}{H_1}-1\right)\frac{x}{L}\right]^n \tag{18}$$

$$n = \frac{\lg(I_2/I_1)}{\lg(H_2/H_1)} \tag{19}$$

When $x=L$, Eq. (18) becomes the following equation

$$I_2/I_1 = (H_2/H_1)^n \tag{20}$$

If we take the logarithm of both sides of the above equation, we can get Eq. (19) after arrangement. Following the same procedure, we can get Eqs. (21) and (22)

$$A_x = A_1\left[1+\left(\frac{H_2}{H_1}-1\right)\frac{x}{L}\right]^{n'} \tag{21}$$

$$n' = \frac{\lg(A_2/A_1)}{\lg(H_2/H_1)} \tag{22}$$

Where A_2 is area of cross section at the big end; A_1 is area of cross section at the small end; A_x is area of cross section at the distance x from the small end; H_2 is depth of cross section at the big end; H_1 is depth of cross section at the small end; I_x is moment of inertia of cross section at the distance x from the small end; L is length of a tapered member; n is 3 for a rectangular section and 2.1～2.6 for an I-shape section; x is the distance from the small end of a tapered element along the longitudinal direction.

In 1962, Fogel and Ketter[9] proposed a method to calculate the deflection of a simply supported member with constant width and varying depth subjected to bending moments. They believed that the yielding section would occur at the position of the largest stress. Timoshenko and Gere[10] also explained that the first yielding section would happen at the location of the largest stress by using a cantilever beam subjected to a concentrated load at the free end. Chen and Lui[11] explained the C_m factors for many uniform members with different boundary conditions and loading types. Hence, the maximum bending moment in a member can be represented. However, these methods are used for a single member only. Members in frames are not always simply supported. Nevertheless, it is very

difficult and almost impossible to find out the location of the maximum stress in a cross section for a beam-column by using the analytical method.

Attalla, et al used a simply supported uniform beam subjected to end moments to simulate several beams in different boundary conditions[12]. Referring to their model, a simply supported beam-column subjected to both end moments and an axial load is developed to simulate several beam-columns in different boundary conditions in this paper. The possible maximum stress occurred in a cross section of a tapered element is calculated. Hence, the possible location of a plastic hinge that may form in an element can be detected. Several cases are described below.

4.1 Uniform Beam

When a simply supported uniform beam is subjected to bending moments at both ends, the maximum bending stress usually occurs at the end of a member, no matter the member is bent in single or in double curvature. When a beam is bent in single curvature with two equal bending moments at both ends, the maximum bending stress is the same along a member. The bending stress can be expressed by Eq. (23). Therefore, the plastic hinge will occur at the end of a member usually.

$$\sigma_x = \frac{M_x}{S_x} \tag{23}$$

Where σ_x is bending stress at the distance x from one end; S_x is section modulus at the distance x from one end.

4.2 Uniform Beam-Column

The position of maximum bending moment in a uniform member that is subjected to bending moments and an axial force is at the distance x from one end. The $\bar{x}$ in the original equation[8] is replaced by x in the current Eq. (24). Hence, we get the following equation

$$\tan kx = -\frac{M_A \cos kL + M_B}{M_A \sin kL} \tag{24}$$

Where

$$k = \sqrt{P/(EI)}$$

Eq. (24) can be applied to a single curvature or a double curvature bending. Usually, the plastic hinge may occur at the end of a member in a double curvature bending.

4.3 Tapered Beam

For a rectangular tapered beam with constant width and varying height subjected to bending moments, the moment of inertia of cross section I_x at a distance of x from the small end can be expressed by Eq. (18); the area of cross section A_x can be expressed by Eq. (21). Hence, these equations are suitable for the I-shape section and the rectangular section. The bending moment M_x at the distance of x from the small end can be expressed by Eq. (25)

$$M_x = \frac{M_A + M_B}{L} x - M_A \tag{25}$$

Where M_A is bending moment at the small end; M_B is bending moment at the big end.

By substituting Eq. (25) into Eq. (23), we get

$$\sigma_x = \frac{M_x H_1 (1 + rx/L)/2}{I_1 (1 + rx/L)^n} \tag{26}$$

When $\frac{d\sigma_x}{dx} = 0$, we can find the position x of the maximum bending stress. This location is the most possible place for the formation of a plastic hinge

$$x = \frac{L}{r(n-2)} + \frac{(n-1)M_A L}{(n-2)(M_A + M_B)} \tag{27}$$

4.4 Tapered Beam-Column

For a rectangular tapered beam-column with constant width and varying height subjected to both bending moments and an axial force, when the shear effect is neglected, taking the equilibrium of moments can derive the governing differential equation of this member for M_x. The bending moment M_x as shown in Fig. 7 at a distance of x from one end is expressed in Eq. (28)

$$M_x = Py + M_A - \frac{M_A + M_B}{L} x \tag{28}$$

By substituting Eq. (29) into Eq. (28), we can get Eq. (30)

$$M_x = -EI_x y'' = -EI_1 (1 + r\frac{x}{L})^n y'' \tag{29}$$

$$EI_1 (1 + r\frac{x}{L})^n y'' + Py = \frac{M_A + M_B}{L} x - M_A \tag{30}$$

By defining Eqs. (31)～(33), and substituting them into Eq. (30), we can get Eq. (34)

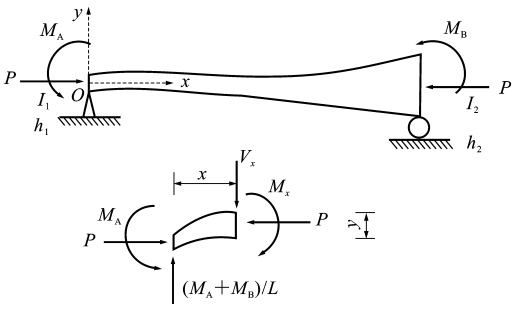

Fig. 7　Tapered Member with Constant Width and Varying Depth Subjected to Bending Moments and Axial Load

图 7　承受弯矩和轴载的变高度楔形构件

$$1+r\frac{x}{L}=\frac{1}{\Omega},\ q=EI_1\frac{r^2}{L^2} \tag{31}$$

$$\frac{\mathrm{d}y}{\mathrm{d}x}=-\Omega^2\frac{r}{L}\frac{\mathrm{d}y}{\mathrm{d}\Omega} \tag{32}$$

$$\frac{\mathrm{d}^2y}{\mathrm{d}x^2}=\frac{r^2}{L^2}\left(2\Omega^3\frac{\mathrm{d}y}{\mathrm{d}\Omega}+\Omega^4\frac{\mathrm{d}^2y}{\mathrm{d}\Omega^2}\right) \tag{33}$$

$$\Omega^{4-n}\frac{\mathrm{d}^2y}{\mathrm{d}\Omega^2}+2\Omega^{3-n}\frac{\mathrm{d}y}{\mathrm{d}\Omega}+\frac{Py}{q}=\frac{M_A+M_B}{qr}\left(\frac{1}{\Omega}-1\right)-\frac{M_A}{q} \tag{34}$$

By multiplying Ω^{n-2} on both sides of Eq. (34), we get Eq. (35)

$$\Omega^2\frac{\mathrm{d}^2y}{\mathrm{d}\Omega^2}+2\Omega\frac{\mathrm{d}y}{\mathrm{d}\Omega}+\Omega^{n-2}\frac{Py}{q}=\Omega^{n-2}\cdot\left[\frac{M_A+M_B}{qr}\left(\frac{1}{\Omega}-1\right)-\frac{M_A}{q}\right] \tag{35}$$

Solving Eq. (35) for y, we get Eq. (36) in the form of Bessel function

$$y=(1+r\frac{x}{L})^{1/2}\{C_1J_{\frac{1}{n-2}}[2\sqrt{\frac{P}{q}}(1+r\frac{x}{L})^{-\frac{n-2}{2}}/(n-2)]+C_2Y_{\frac{1}{n-2}}[2\sqrt{\frac{P}{q}}(1+r\frac{x}{L})^{-\frac{n-2}{2}}/(n-2)]\}+\frac{M_A+M_B}{PL}x-\frac{M_A}{P} \tag{36}$$

By substituting boundary conditions $y(0)=y(L)=0$ into Eq. (36), these constants C_1, C_2 can be determined. Therefore, we get Eq. (37)

$$y=[\frac{M_A}{P}(1+r)^{\frac{1}{2}}Y_{\frac{1}{n-2}}(U)+\frac{M_B}{P}Y_{\frac{1}{n-2}}(V)]J_{\frac{1}{n-2}}(W)\{(1+r)^{\frac{1}{2}}\cdot[J_{\frac{1}{n-2}}(V)Y_{\frac{1}{n-2}}(W)+J_{\frac{1}{n-2}}(W)Y_{\frac{1}{n-2}}(V)]\}^{-1}-[\frac{M_B}{P}J_{\frac{1}{n-2}}(V)+\frac{M_A}{P}(1+r)^{\frac{1}{2}}J_{\frac{1}{n-2}}(U)]Y_{\frac{1}{n-2}}(W)\cdot\{(1+r)^{\frac{1}{2}}[J_{\frac{1}{n-2}}(V)Y_{\frac{1}{n-2}}(W)+J_{\frac{1}{n-2}}(W)Y_{\frac{1}{n-2}}(V)]\}^{-1}+\frac{M_A+M_B}{PL}x-\frac{M_A}{P} \tag{37}$$

Where

$$U=2\sqrt{\frac{P}{q}}(1+r)^{-\frac{n-2}{2}}(n-2)^{-1};$$

$$V=2\sqrt{\frac{P}{q}}(n-2)^{-1};$$

$$W=2\sqrt{\frac{P}{q}}(1+r\frac{x}{L})^{-\frac{n-2}{2}}(n-2)^{-1}.$$

The parameter r in Eq. (37) is equal to r_1 for an I-shape section. By substituting Eq. (37) into Eq. (28), we can get the bending moment M_x at a distance x from the small end. When we substitute the axial force P and the bending moment M_x into Eq. (38), we can have the bending stress σ_x. However, it is very difficult to differentiate Eq. (38) to get the position of the maximum bending stress

$$\sigma_x=\frac{P}{A_x}+\frac{M_x}{S_x} \tag{38}$$

Where P is axial force; A_x is cross-sectional area at the distance x from the small end; M_x is bending moment at the distance x from the small end.

Hence, we do not differentiate Eq. (38) directly. We set $\sigma_x=\sigma_y$ in Eq. (38) in order to express the yielding of a section. By dividing σ_y on both sides of Eq. (38), we get the following equation

$$\frac{P}{P_{yx}}+\frac{M_x}{M_{yx}}=1 \tag{39}$$

Where P_{yx} is squash load at a distance of x from the small end; M_{yx} is initial yielding moment at a distance of x from the small end.

Once a plastic hinge occurs at the nodal point of an element, ten separately observational points will be set up at equal distance along the element. The axial load P and bending moment M_x obtained from Eq. (37) and Eq. (28) at each observational point will be calculated and substituted into Eq. (39). The summation of the axial load ratio and moment ratio in Eq. (39) will be computed for each observational point. In other words, the value of Z_i is calculated from Eq. (40)

$$Z_i=\frac{P}{P_{yx}}+\frac{fM_x}{M_{px}} \tag{40}$$

The location of the largest value of Z_i in these ten observational points is the most possible place where a plastic hinge may occur firstly. Hence, an additional nodal point will be inserted at this place.

If we calculate the value of Z_u based upon the following Eq. (41) that is respected to the limit surface

$$Z_u = \frac{P}{P_{yx}} + \frac{M_x}{M_{px}} \tag{41}$$

We can also get the possible location of a plastic hinge that may form in an element. However, it is more accurate when Z_i is used in the prediction of the possible location of a plastic hinge.

5 Numerical Examples

The most possible location of a plastic hinge in a tapered member by the proposed method is demonstrated by several numerical examples in this section. In every incremental load step, the limit surface is used to check the internal nodal forces of each nodal point. The incremental load applied on the structure is scaled down when the plastic hinge is going to form in a tapered member. Hence, we can guarantee that when a plastic hinge just forms in a tapered member, the applied incremental load is not overloaded. Several load and deflection curves of tapered members or frames with tapered members are analyzed by the proposed method. These plastic limit loads of frames with tapered members are also discussed in these numerical examples. The lowest limit load of a frame with tapered members can be found by setting a new nodal point at the most possible position of a plastic hinge.

5.1 Example 1

A tapered cantilever beam of rectangular section with constant width is subject to a horizontal load at the free end. The lateral load is increased until the beam as shown in Fig. 8 is destroyed. The most possible location of a plastic hinge in this beam is detected by the proposed method. The relation of load and deflection is analyzed by the simple plastic hinge method.

As shown in Fig. 8, curve (1) is the result by taking only one element for the beam. According to Eq. (27), the possible location of plastic hinge detected by the proposed method is 127 cm from the fixed end. Curve (2) is the result when a new

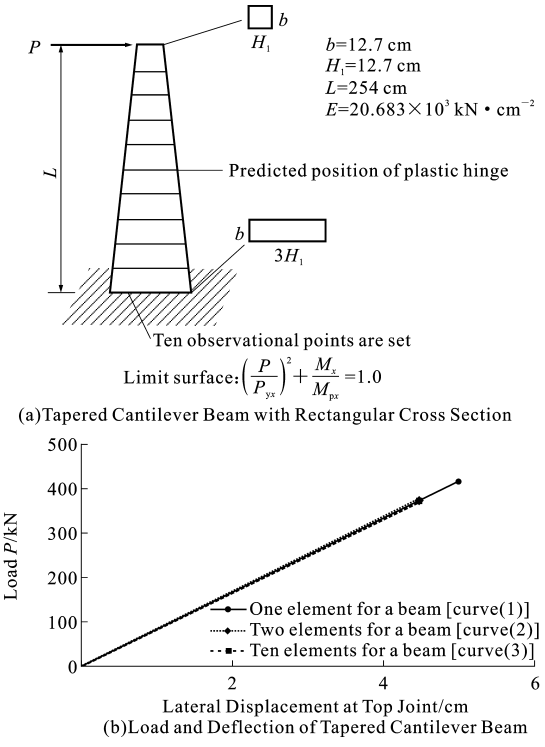

Fig. 8 Load and Deflection of Tapered Cantilever Beam with Rectangular Cross Section

图 8 矩形截面楔形悬臂梁的荷载-挠度

nodal point is added at the most possible location of a plastic hinge detected by the proposed method. Curve (3) is the result when the cantilever beam is divided into ten equal elements. The limit load that is predicted by curve (1) is higher than that predicted by both curve (2) and curve (3). It implies that limit load of a tapered beam is overestimated about 13% when only one element is used in analysis. Limit loads predicted by curve (2) and curve (3) are the same. However, in curve (2) only two elements are used by the proposed method.

5.2 Example 2

An I-shape beam-column with constant width and varying depth is shown in Fig. 9. The column height L is 352.55 cm. The depth of the small end H_1 is 15.24 cm. The big end's depth H_2 is 106.68 cm. The flange width b_f is 20.32 cm. The web thickness t_w is 0.72 cm. The flange thickness t_f is 1.1 cm. The elastic modulus E is 206 84 kN·cm^{-2}. The yielding stress σ_y is 24.8 kN·cm^{-2}. The vertical load P of 889.6 kN is applied first and kept constant. The axial load P divided by the squash load P_y of the small end is 0.66. The axial

load P divided by the squash load P_y of the big end is 0.3. The lateral load H is applied and increased till the member collapses.

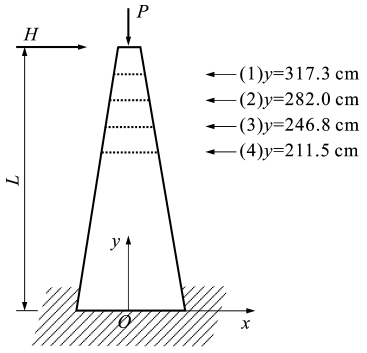

Fig. 9　Tapered Beam-Column of I-Section

图 9　工形截面楔形梁柱

In this example, we try to find the correct load and deflection relation curve by using the fewer elements. One element is taken for the beam-column at first. A plastic hinge will be formed at the fixed end after analysis. Hence, one element that includes ten observational points is used for the beam-column analysis. These first four observational points are shown in Fig. 9. The value of Z_i in Eq. (40) is calculated for each observational point. The largest value of Z_i of these observational points represents the most possible location of a plastic hinge. Point (2) is at the predicted location of a plastic hinge. Hence, two elements are used for the beam-column analysis after a new nodal point is added at point (2).

In Fig. 10, curve (a) is the result by using only one element for this member. Curve (b) is the result by using two elements for this member with a new nodal point at point (1). Curve (c) is the result by using two elements for this member with a new nodal point at point (2). Curve (d) is the result by using two elements for this member with a new nodal point at point (3). Curve (e) is the result by using two elements for this member with a new nodal point at point (4).

The value of Z_i at point (2) in curve (c) is 1.134. The value of Z_i at point (1) in curve (b) is 1.113. The value of Z_i at point (3) in curve (d) is 1.072. The value of Z_i at point (4) in curve (e) is 0.994. The value of Z_i in curve (c) is the largest

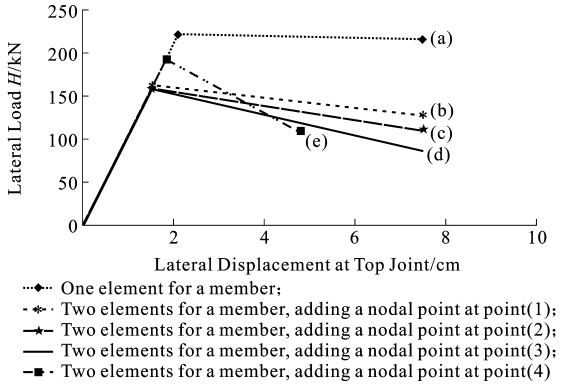

Fig. 10　Load and Deflection of Tapered I-Section Beam-Column

图 10　工形截面楔形梁柱的荷载-挠度

one among curves (a) through (e). The limit load of curve (d) is the lowest one. However, the limit load of curve (c) is very close to that of curve (d).

The limit load of curve (d) is only 1% lower than that of curve (c) as shown in Fig. 10. The actual location of a plastic hinge may be very close to point (2). This example demonstrates that the proposed method can predict for the most possible location of a plastic hinge in a tapered member. After the nodal point (2) is added into the tapered member, the limit load of the beam-column reduces 39% as compared to that by using only one element for a member. It is seen that the limit load of a tapered beam-column is always overestimated if the possible location of a plastic hinge is not found correctly.

5.3　Example 3

A portal frame as shown in Fig. 11 composes two tapered columns and one uniform beam. These columns have a constant width but a linearly tapered depth. All members have I-shape sections. The bottom of column is hinged. The span L of each member is 355.6 cm. The web thickness t_w of an I-shape section is 0.72 cm. The flange thickness t_f of an I-shape section is 1.1 cm. The flange width b_f of an I-shape section of beam and columns is 30.48 cm. The depth H_1 or H_2 of the uniform beam is the same of 76.2 cm. The depth H_1 of the small end of the tapered column is 15.24 cm. The depth H_2 of the big end of the tapered column is 91.44 cm. Young's modulus E is 20 684 kN · cm^{-2}. The

yielding stress σ_y is 24.8 kN · cm^{-2}. The plastic hinge is not permitted to occur in this beam on purpose when the size of beam is selected. The vertical load P is 889.6 kN. The value of P is equal to $0.66P_y$ at the small end of column; while the value of P is equal to $0.33P_y$ at the big end of column. These vertical loads P are applied first and kept constant. Then, the horizontal load H is applied and increased from zero to the limit load till the portal frame is going to collapse.

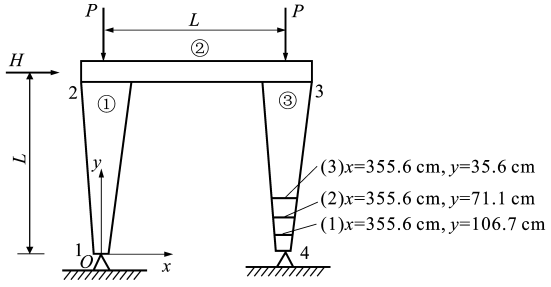

Fig. 11 Portal Frame Dimensions and Three Observational Points

图 11 门式框架尺寸

If one element is taken for each member, there are four nodal points. After an initial analysis, a plastic hinge is formed firstly at the nodal point (3) in the third element. Therefore, ten observational points are set in the third element in order to compute Z_u and Z_i. Because Z_u and Z_i become small after the fourth observational point, these first three values of Z_u and Z_i are shown in Fig. 12 respectively.

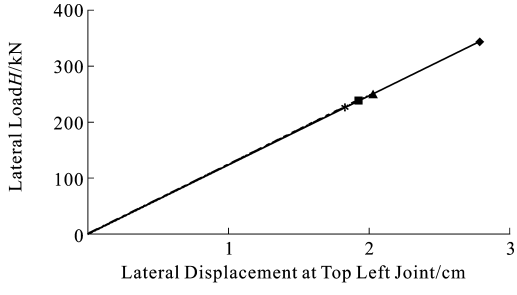

Fig. 12 Load and Deflection of Portal Frame

图 12 门式框架的荷载-挠度

It is found that the largest value of Z_i is at the second observational point. It means that a possible plastic hinge will be formed at the second observational point. Hence, a new nodal point is added at the second observational point. Now, there are five nodal points and four elements for the portal frame analysis. The load and deflection curve (c) is the result of analysis when a new nodal point is added at the second observational point. The limit load of curve (c) is the lowest one of several analyses.

The largest value of Z_u is at point (1) that is corresponding to curve (b). However, the limit load of curve (b) is not the lowest one. Therefore, the checking criteria by using Z_i are better than that by using Z_u. The limit load of curve (a) is higher than that of curve (c) about 49%. This result represents the proposed method is acceptable and reasonable. The actual location of plastic hinge is very close to the second observational point.

6 Conclusions

(1) The stiffness matrixes of three rectangular sections successfully superpose the stiffness matrix of a tapered member of I-shape section in this paper. It is shown that the stiffness matrix of a tapered member of I-shape section is reasonable and correct by that process of superposition.

(2) In order to find a possible location of plastic hinge in a tapered member, the checking criteria by using Z_i are better than that by using Z_u. Z_i is calculated by using the left side of the equation of the initial yielding surface. Z_u is calculated by using the left side of the equation of the limit surface.

(3) The plastic limit load is overestimated if only one element is used for a tapered member. The proposed method to predict the approximate position of a plastic hinge in a tapered member is effective and accurate. When the possible location of a plastic hinge in a tapered member is found, a new nodal point at that location can be set. The fewer elements can be used to reasonably predict behavior for structures with tapered members.

(4) For the examples studied in this paper, the error of limit load for a beam-column may be up to

49%. These errors of limit loads of beam-columns are more serious than that of beams, if these predicting locations of plastic hinges in tapered members are incorrect.

References:

[1] HAYALIOGLU M S, SAKA M P. Optimum Design of Geometrically Nonlinear Elastic-Plastic Steel Frames with Tapered Members[J]. Computers and Structures, 1992, 44(4): 915-924.

[2] FERTIS D G, KEENE M E. Elastic and Inelastic Analysis of Nonprismatic Member[J]. Journal of Structural Engineering, ASCE, 1990, 116(2): 475-489.

[3] MOHAMED S E, KOUNADIS A N, SIMITSES G J. Elasto-Plastic Analysis of Gabled Frames with Nonprismatic Geometries[J]. Computers and Structures, 1992, 44(3): 693-697.

[4] KING W S, CHEN W F. Practical Second-Order Inelastic Analysis of Semi-rigid Frames[J]. Journal of Structural Engineering, ASCE, 1994, 120(7): 2 156-2 175.

[5] DUAN L, CHEN W F. A Yield Surface Equation for Doubly Symmetrical Section[J]. Engineering Structures, 1990, 12(2): 114-119.

[6] CHEN W F, ATSUTA T. Theory of Beam-Columns, in-Plane Behavior and Design[M]. New York: McGraw-Hill Book Co., 1976.

[7] CHEN C J. The Elastic-Plastic Analysis of Frames with Tapered Members[D]. Tooyuan: Chung Cheng Institute of Technology, 1995.

[8] GERE J M, CARTER W O. Critical Buckling Loads for Tapered Columns[J]. Journal of the Structural Division, ASCE, 1962, 88(S1): 1-11.

[9] FOGEL C M, KETTER R L. Elastic Strength of Tapered Columns[J]. Journal of the Structural Division, ASCE, 1962, 88(S5): 67-106.

[10] TIMOSHENKO S P, GERE J M. Mechanics of Materials[M]. Belmont: Wadsworth Inc, 1984.

[11] CHEN W F, LUI E M. Structural Stability: Theory and Implementation[M]. New York: Elsevier Science Publishing Co., 1987.

[12] ATTALLA M R, DRIERLEIN G G, MCGUIRE W. Spread of Plasticity: Quasi-Plastic-Hinge Approach[J]. Journal of Structural Engineering, ASCE, 1994, 120(8): 2 451-2 473.